Journal of Hazardous Materials 171 (2009) 640–646

Contents lists available at ScienceDirect

Journal of Hazardous Materials

journal homepage: www.elsevier.com/locate/jhazmat

Adsorption of Hg^{2+} from aqueous solution onto polyacrylamide/attapulgite

Yijiang Zhao[a,*], Yan Chen[a,b], Meisheng Li[a], Shouyong Zhou[a], Ailian Xue[a], Weihong Xing[b]

[a] Chemistry Department of Huaiyin Teachers College, Key Laboratory for Chemistry of Low-Dimensional Materials of Jiangsu Province, No. 111 Changjiang West Road, Huaian 223300, Jiangsu Province, PR China
[b] State Key Laboratory of Materials-Oriented Chemical Engineering, Nanjing University of Technology, No. 5 Xinmofan Road, Nanjing 210009, Jiangsu Province, PR China

ARTICLE INFO

Article history:
Received 4 December 2008
Received in revised form 30 May 2009
Accepted 11 June 2009
Available online 18 June 2009

Keywords:
Attapulgite
Polyacrylamide
Mercury adsorption
Kinetics
Isotherm

ABSTRACT

Polyacrylamide/attapulgite (PAM/ATP) was prepared by the solution polymerization of acrylamide (AM) onto γ-methacryloxypropyl trimethoxy silane (KH-570)-modified attapulgite (ATP). PAM/ATP was characterized using Fourier transform infrared (FTIR) and X-ray photoelectron spectroscopy (XPS). The effects of contact time, adsorbent dosage, and pH of the initial solution on the adsorption capacities for Hg^{2+} were investigated. The adsorption process was rapid; 88% of adsorption occurred within 5 min and equilibrium was achieved at around 40 min. The equilibrium data fitted the Langmuir sorption isotherms well, and the maximum adsorption capacity of Hg^{2+} onto PAM/ATP was found to be 192.5 mg g^{-1}. The adsorption kinetics of PAM/ATP fitted a pseudo-second-order kinetic model. Our results suggest that chemisorption processes could be the rate-limiting steps in the process of Hg^{2+} adsorption. Hg^{2+} adsorbed onto PAM/ATP could be effectively desorbed in hot acetic acid solution, and the adsorption capacity of the regenerated adsorbents could still be maintained at 95% by the sixth cycle.

1. Introduction

Mercury is one of the most toxic metals. Due to its toxicity and bioaccumulation within the food chain, only extremely low levels of Hg^{2+} are tolerated in the environment [1]. It is also well known that Hg^{2+} has a very high tendency to bind to proteins, mainly causing damage to the renal and nervous systems [2]. In order to monitor and prevent Hg^{2+} pollution, a number of different technologies, such as precipitation [3,4], biosorption [5], membrane filtration [6], ionic exchange [7] and solvent extraction [8], have been used for the sequestering of Hg^{2+} from wastewater. However, these techniques are associated with problems such as excessive time requirements, high costs, inefficiency, and energy use.

Attapulgite (ATP, or palygorskite) is a kind of crystalline hydrated magnesium aluminum silicate mineral. Its ideal structure was studied by Bradley in 1940 and is shown in Fig. 1 [9]. Presently, ATP and activated ATP, which is a natural, cheap, adsorbent clay mineral with exchangeable cations and reactive-OH groups on its surface [10], have been intensively used as adsorbents for the removal of heavy metal ions and organic contaminants [11–16]. In order to enhance its adsorption capacity and selectivity, ATP has recently been widely treated with some organic reagents, such as 2,2-bis(hydroxymethyl)propionic acid [17], octodecyl trimethyl ammonium chloride [18], and ammonium citrate tribasic [19].

Polyacrylamide (PAM), a water-soluble polymer with large numbers of amide side groups, has been successfully grafted onto the surfaces of various matrices as selective sorbents for the removal of Hg^{2+} from aqueous solution [20–26]. The amide groups on the flexible PAM graft chains should provide the opportunity for rapid interaction with aqueous Hg^{2+} to form mercury-amide linkages [21]. Nevertheless, the adsorption of Hg^{2+} onto polyacrylamide/attapulgite (PAM/ATP), which is PAM grafted on the surface of γ-methacryloxypropyl trimethoxy silane (KH-570)-modified ATP by solution polymerization, is still scarcely used.

In this study, we prepared a new kind of PAM/ATP adsorbent composite by solution polymerization. The coupling reagent KH-570 was used to introduce ethylene groups onto the ATP surface, and PAM was then grafted onto the KH-570-modified ATP. The effects of contact time, adsorbent dosage, and pH of the initial solution on the removal of Hg^{2+} were studied. The experimental equilibrium adsorption data were analyzed using Langmuir isotherm models, and the kinetics and the factors controlling the adsorption process were investigated. The mechanisms of adsorption of Hg^{2+} onto PAM/ATP were identified by X-ray photoelectron spectroscopy (XPS) analysis.

2. Materials and methods

2.1. Materials and reagents

The ATP was supplied by Jiangsu Xuyi Anhalt Nonmetallic Mining Ltd. with an average diameter of 200 mesh.

* Corresponding author. Tel.: +86 517 83525021; fax: +86 517 83525028.
E-mail address: cyjzhao@yahoo.com (Y. Zhao).

0304-3894/$ – see front matter © 2009 Elsevier B.V. All rights reserved.
doi:10.1016/j.jhazmat.2009.06.048

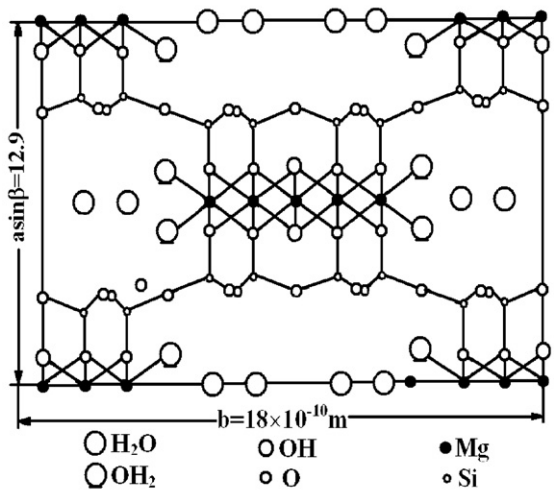

Fig. 1. Crystalline structure of ATP from (0 0 1) plane.

γ-Methacryloxypropyl trimethoxy silane (KH-570) was provided by Nanjing Shuguang Chemical Group Co. Acrylamide (AM) was provided by Guoyao Group of Chemical Reagents Ltd. 2,2′-Azo-bis-iso-butyronitrile (AIBN) was provided by Shanghai Chemical Co., Ltd. He Wei four test. All other chemicals used in this study were of analytical grade. The Hg^{2+} aqueous solution was prepared with $Hg(NO_3)_2$. Distilled water was used in all experiments.

2.2. Polymerization of AM on ATP by solution polymerization

The coupling reagent KH-570 was used to introduce ethylene groups onto the ATP surface before the graft polymerization was initiated with AIBN. The ethylene groups could then be used to polymerize with AM. The preparation of PAM/ATP is shown schematically in Scheme 1. The grafting process was as follows: 1.0 mL distilled water and 3.0 g ATP (dried at 105 °C) were successively dispersed in 100 mL toluene, and 3.0 mL KH-570 was then added and dissolved with the help of ultrasonic agitation for 40 min in a 250 mL flask. The mixture was then refluxed with electromagnetic stirring at 45–50 °C for 4 h. Finally, the ATP immobilized on the KH-570 was separated by filtration and rinsed, first with toluene and ethanol, and then washed thoroughly with distilled water. The KH-570-modified ATP was dried in a desiccator at 105 °C.

KH-570-modified ATP (2.0 g) was added to a 250-mL Wolff bottle containing 100 mL of the toluene solution and stirred at room temperature. Then 0.6 g AM and 0.06 g AIBN were successively added. The mixture was then refluxed with stirring at 80 °C for 6 h under N_2 atmosphere. Finally, the resulting PAM/ATP was separated and washed with toluene, ethanol, and distilled water in sequence, dried in a desiccator at 105 °C, and then stored in the desiccator for subsequent analyses or adsorption experiments.

2.3. Metal adsorption experiments

All the adsorption experiments were carried out in 250-mL iodine flasks by adding a given amount of PAM/ATP to 40 mL of aqueous Hg^{2+} solution and shaking in a shaking thermostatic bath (SHZ-B, China) at 170 rpm at 30 °C, for a given time. Hg^{2+} solution was prepared using $Hg(NO_3)_2$. Adsorption isotherms and the effects of the initial concentration were studied in the range of 100–900 ppm. The effects of adsorbent mass were studied in the range of 0.05–0.9 g. The effects of pH were studied in the range of 0.99–6.5, with 0.1 M HNO_3 and NaOH used as pH controls. Kinetics and the effects of contact time on adsorption were determined in the range of 5–120 min. After adsorption, the solid and liquid phases were separated by centrifugation at 2000 rpm for 15 min. All of the initial and final Hg^{2+} concentrations in the solution samples were determined using inductively coupled plasma optical emission spectroscopy (ICP-OES, PE 2000DV). The degree of adsorption was calculated based on the differences between the aqueous Hg^{2+} concentration before and after adsorption, according to the following equation:

$$Q = \frac{C_i V_i - C_f V_f}{m} \quad (1)$$

where Q is the metal uptake capacity (mg g^{-1}), C_i is the initial metal concentration (mg L^{-1}), V_i is the initial volume (L), C_f is the final metal concentration (mg L^{-1}), V_f is the final volume (L) and m is the dry weight of the PAM/ATP added into the flask.

2.4. Regeneration of the sorbent

After the adsorption experiments, the Hg^{2+}-loaded samples (0.15 g) were left in contact with 40 mL 80% acetic acid and shaken in an orbital shaker, operated at 60 °C for 30 min. After adsorption, the solid and liquid phases were separated by centrifugation at 2000 rpm for 15 min. All of the initial and final Hg^{2+} concentrations in the solution samples were determined by ICP-OES. To determine the reusability of the PAM/ATP, consecutive adsorption–desorption cycles were repeated six times under the same conditions.

2.5. Characterization

The structures of the ATP, KH-570-modified ATP, PAM/ATP, AM and KH-570 were characterized using a Nicolet Corporation AVATAR-360FT-IR spectrophotometer (USA) to elucidate the reaction mechanisms. XPS analyses were performed using an ESCALAB 250 spectrophotometer with an Al Kα X-ray source (1486.6 eV of photons). The binding energies (BEs) were calibrated by the C 1s peak at 284.6 eV.

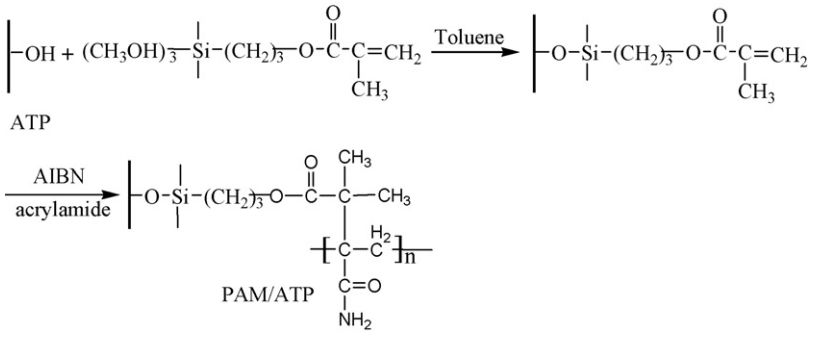

Scheme 1. The preparation procedure to PAM/ATP.

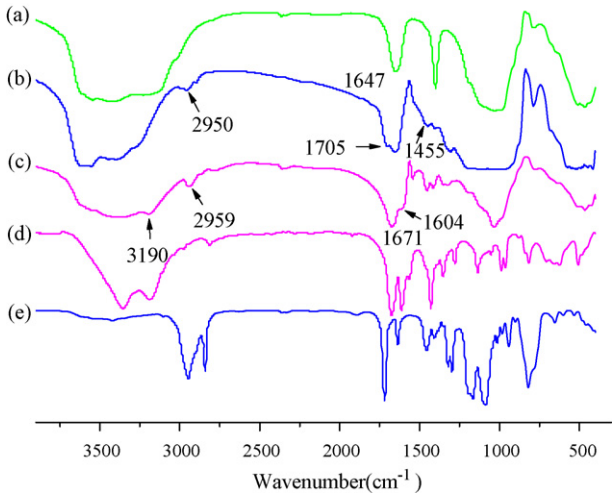

Fig. 2. FTIR spectra of (a) ATP; (b) KH-570-modified ATP; (c) PAM/ATP; (d) AM; and (e) KH-570

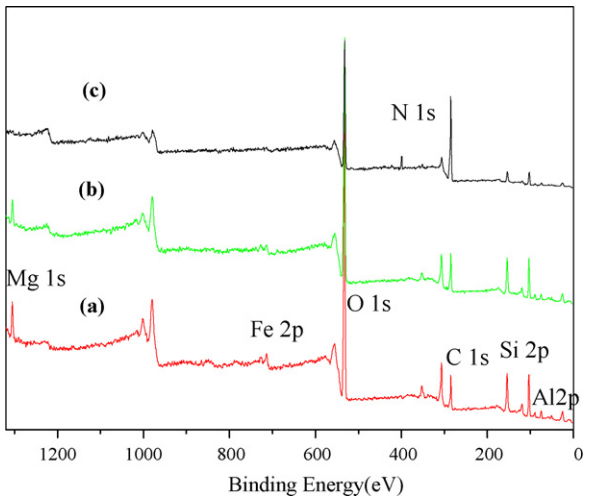

Fig. 3. Typical wide-scan XPS spectra of (a) ATP; (b) KH-570-modified ATP; and (c) PAM/ATP.

3. Results and discussion

3.1. Surface structure

3.1.1. Infrared spectrum

Fig. 2 shows the FTIR spectra of ATP, KH-570-modified ATP, PAM/ATP, AM and KH-570. The new peaks at 1705 and 1455 cm^{-1} for KH-570-modified ATP (Fig. 2b) are usually representative of the carboxyl group (–COO–) and C=C group, suggesting that the silane coupling agent reacted successfully with the –OH groups of ATP, which is also indicated in Scheme 1. Absorption peaks at 2950 cm^{-1} in Fig. 2b and at 2959 cm^{-1} in Fig. 2c, correspond to the –C–H stretching of KH-570 and AM. The peaks at 1604 and 3190 cm^{-1} (Fig. 2c) correspond to the bending and stretching vibrations of the $-NH_2$ group, respectively. The peak for the carboxyl group at 1705 cm^{-1} in Fig. 2b for the KH-570-modified ATP is no longer observed in the PAM/ATP spectrum, possibly due to coverage of the surface with PAM. Moreover, the FTIR spectrum for PAM/ATP shows a major peak at 1671 cm^{-1} in Fig. 2c, corresponding to the C=O stretching vibration of the amide group ($-CONH_2$) [27], indicating successful grafting of PAM on the surface of the ATP. Therefore, the FTIR spectra in Fig. 2 clearly support the surface modification reactions illustrated in Scheme 1.

3.1.2. XPS spectrum

To show that PAM can be successfully grafted onto the surfaces of the ATP, XPS analyses were conducted to determine the surface element composition. The changes in surface C 1s, Si 2p, Al 2p, Fe 2p, Mg 1s, O 1s and N 1s element contents were demonstrated by XPS surface analyses of the ATP, KH-570-modified ATP, and PAM/ATP (Fig. 3 and Table 1). It can be clearly seen that the carbon content increased from 15.02% to 51.54%. However, the oxygen, silicon, magnesium, iron and aluminum contents decreased. Moreover, a new peak for N 1s at a BE of 399.61 eV became visible for PAM/ATP. These results confirm that PAM was successfully grafted onto the surface of the KH-570-modified ATP via the mechanism shown in Scheme 1.

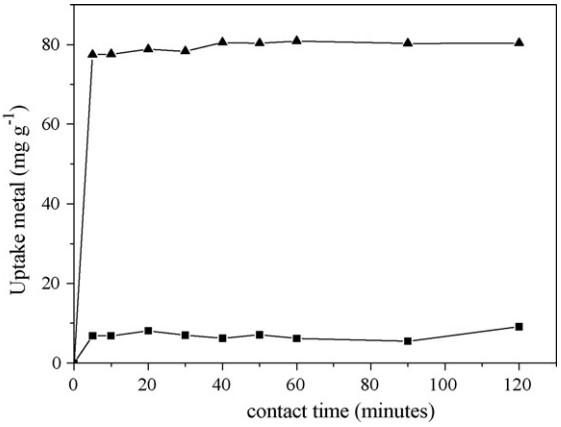

Fig. 4. Effect of shaking time on adsorption of ATP(■) and PAM/ATP(▲) for Hg^{2+} (concentration of initial solution 327.7 mg L^{-1}, amount of PAM/ATP 0.15 g, pH of initial suspension 4.40).

3.2. Adsorption of Hg^{2+} ions

3.2.1. Effect of contact time

Fig. 4 shows the removal of Hg^{2+} from aqueous solution by ATP and PAM/ATP as a function of contact time. The adsorption of Hg^{2+} onto PAM/ATP was very rapid (Fig. 4) with an increase in contact time from 0 to 5 min, and sorption equilibration was achieved by 40 min, followed by a constant adsorption rate with further shaking time. This was due to the high complexation rate between Hg^{2+} ions and reactive function groups on the surface of PAM/ATP. According to studies on hard and soft metals, soft metal Hg forms more stable bonds with nitrogen-containing (soft) ligands [28], and the fast reaction can be ascribed to the flexibility of the dangling PAM chains in the water [23]. It should be noted that adsorption is not a diffusion-controlled process. At the same time, although the adsorption of Hg^{2+} onto ATP is also very fast, the amount of Hg^{2+} adsorbed per unit weight of adsorbent is much smaller than onto

Table 1
Data of element content from XPS full-scan spectra.

Samples	O 1s (%)	C 1s (%)	Si 2p (%)	Mg 1s (%)	Fe 2p (%)	Al 2p (%)	N 1s (%)
ATP	61.19	15.02	15.04	3.23	2.11	3.41	0
KH-570-modified ATP	58.85	19.44	14.76	2.24	1.75	2.97	0
PAM/ATP	35.53	51.54	6.36	0.28	0.73	1.33	4.23

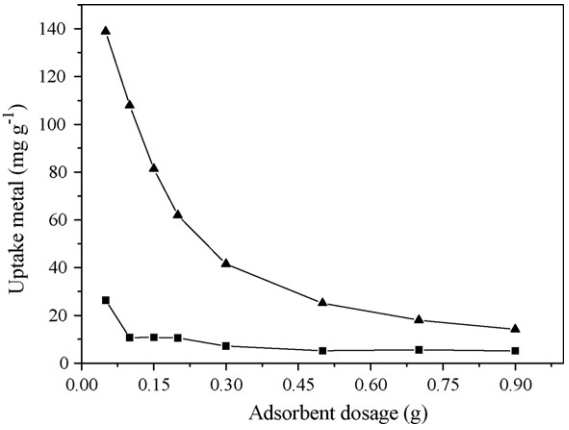

Fig. 5. Effect of amount of adsorbent on adsorption of ATP(■) and PAM/ATP(▲) for Hg^{2+} (concentration of initial solution 327.7 mg L^{-1}, contact time 40 min, pH of initial suspension 4.40).

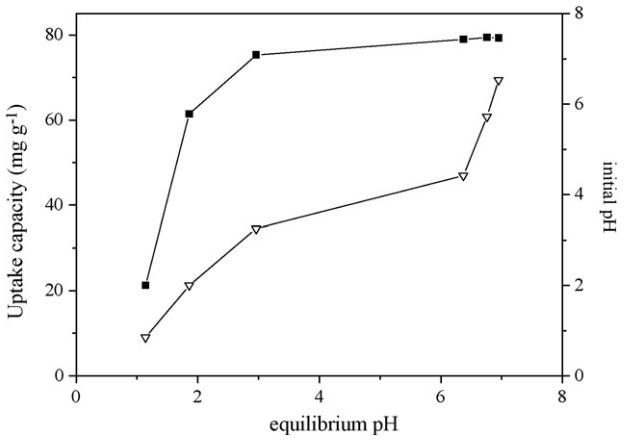

Fig. 6. Effect of pH of the equilibrium solution on adsorption of PAM/ATP for Hg^{2+} (uptake capacity: ■; initial pH: ▽; concentration of initial solution 327.7 mg L^{-1}; contact time 40 min; amount of PAM/ATP 0.15 g).

PAM/ATP, indicating that the PAM grafted onto the surface of ATP can enhance the adsorption of Hg^{2+} ions.

3.2.2. Effect of adsorbent dosage

The amount of adsorbent is an important parameter, because this reflects the adsorption capacity of an adsorbent, for a given initial concentration of the adsorbate. Fig. 5 shows the amounts of Hg^{2+} removal by ATP and PAM/ATP at various different adsorbent dosages. The Hg^{2+} uptake decreased with increasing amounts of ATP and PAM/ATP. On the other hand, the amounts of Hg^{2+} adsorbed per unit weight of ATP or PAM/ATP, i.e., the adsorption efficiency of ATP or PAM/ATP, decrease with increasing amount of ATP or PAM/ATP.

As shown in Fig. 5, the Hg^{2+} adsorbed per g of ATP/PAM decreased more rapidly than for ATP, with increasing adsorbent dosages. At the same time, the amount of Hg^{2+} adsorbed per unit weight of PAM/ATP was greater than that for ATP at the same adsorbent dosage. These differences can be explained by the fact that PAM/ATP contains large numbers of adsorption sites (amide groups) on its surface, while ATP does not. Hg^{2+} is assumed to be able to form a covalent bond with the amide group (i.e., amido-Hg) in solution by replacing a hydrogen atom from the amide group [23]. Considering the cost and efficiency of wastewater treatment, 0.15 g was used as a suitable dosage for the rest of the batch experiments.

3.2.3. Effect of pH of solution

The pH of the aqueous solution is an important parameter in the adsorption process [29]. The influence of pH of the equilibrium suspension on adsorption capacity of Hg^{2+} using PAM/ATP was therefore studied, within the pH range of 1.0–7.0 (Fig. 6). Precipitation of Hg^{2+} did not occur throughout the entire pH range, as shown in Fig. 6 [30]. Adsorption of Hg^{2+} increased with increasing equilibrium pH and reached almost maximum adsorption around an equilibrium pH value of 6.4. In other words, the pH value of the initial suspension is 4.4. Adsorption was then maintained at about the same level within the equilibrium pH range of 6.4–7.0. This also suggests that PAM/ATP exhibited a low affinity for Hg^{2+} at initial pH < 2, and a higher affinity between initial pH 4.4 and 6.5. This also suggests that the Hg^{2+} linkage proceeds with deprotonation of the amide groups [24]. Thus, increasing pH of the initial solution favors Hg^{2+}-amide linkage formation between the reactive groups on the PAM/ATP and Hg^{2+}. Hence, initial solutions with pH 4.4 were used in our experiments.

XPS spectra are widely used to identify the existence of a particular element in a material [31]. Fig. 7 shows typical XPS spectra for PAM/ATP before and after Hg^{2+} adsorption. Hg^{2+} is clearly present on the surface of PAM/ATP after the Hg^{2+} adsorption experiment.

3.2.4. Equilibrium adsorption of Hg^{2+}

The adsorption capacity of PAM/ATP for Hg^{2+} was investigated over a range of metal concentrations. The adsorption data can often be modeled by the Langmuir isotherm equation [32] as:

$$q_e = \frac{q_m K_L C_e}{1 + K_L C_e} \quad (2)$$

in which q_m is the maximum amount of adsorption (mg g^{-1}), q_e is the equilibrium capacity of Hg^{2+} on the adsorbent (mg g^{-1}), C_e is the equilibrium concentration of Hg^{2+} in the solution (mg L^{-1}), and K_L is the adsorption equilibrium constant (L mg^{-1}). The experimental adsorption isotherm results for Hg^{2+} on PAM/ATP at pH 4.4 at different initial Hg^{2+} concentrations are shown in Fig. 8. In general, Hg^{2+} uptake by PAM/ATP increased with increasing initial Hg^{2+} concentrations. It also appears that the adsorption isotherm results for PAM/ATP can be well described by the Langmuir equation. This may be due to a homogeneous distribution of active sites on the PAM/ATP surface. According to the equation, the maximum adsorption capacity (q_m) of Hg^{2+} on PAM/ATP was 192.5 mg g^{-1} (r^2 = 0.991). Similar findings for Hg^{2+} adsorption from aqueous solutions have been reported in other studies [20,33].

The essential characteristic of the Langmuir equation can be expressed in terms of a dimensionless constant separation factor or equilibrium parameter R_L, which was defined by McKay et al.

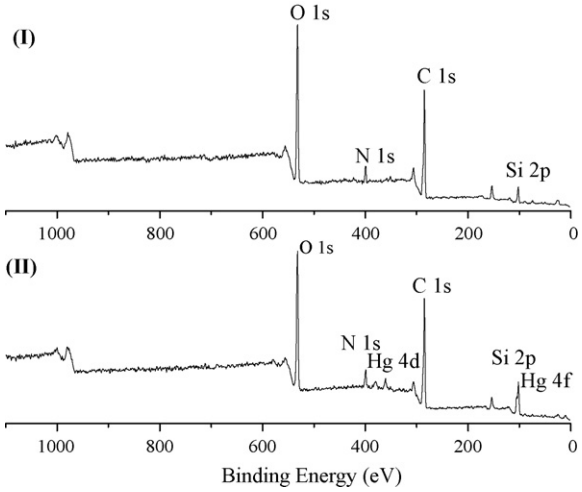

Fig. 7. Typical XPS spectra of PAM/ATP: (I) before Hg^{2+} adsorption; (II) after Hg^{2+} adsorption.

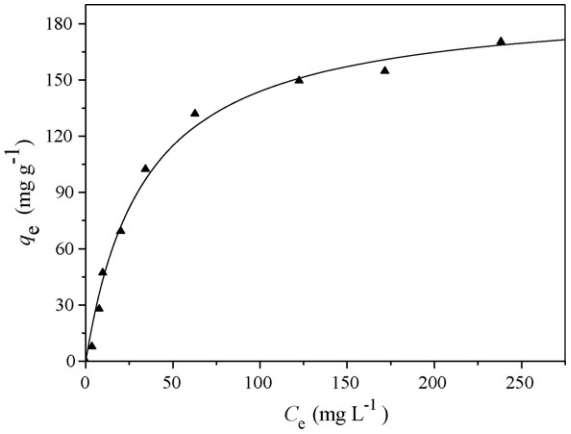

Fig. 8. Hg^{2+} adsorption isotherms on PAM/ATP: experimental equilibrium uptakes and the Langmuir model fitting (pH of initial suspension 4.40, contact time 40 min, amount of PAM/ATP 0.15 g).

[34] as:

$$R_L = \frac{1}{(1 + K_L C_0)} \quad (3)$$

where C_0 is the highest initial metal concentration (mg L^{-1}) and K_L is the same as above. The value of R_L indicates the nature of the adsorption process to be either unfavorable ($R_L > 1$), linear ($R_L = 1$), favorable ($0 < R_L < 1$) or irreversible ($R_L = 0$).

In this study, the low value of R_L ($R_L = 0.0371$) indicates favorable adsorption. Hence, the q_m, K_L and R_L values indicate that PAM/ATP exhibits good potential for the adsorption of Hg^{2+}.

3.2.5. Adsorption dynamics

In order to examine the mechanisms controlling Hg^{2+} adsorption on PAM/ATP, such as mass transfer and chemical reactions, the experimental data were tested using pseudo-first-order and pseudo-second-order kinetic equations. The pseudo-first-order kinetic model was suggested by Lagergren [35] for the adsorption of solid/liquid systems and its formula is given as:

$$\log(q_e - q_t) = \log q_e - \frac{k_1}{2.303} t \quad (4)$$

Eq. (4) can be transformed into nonlinear forms, which can be used to predict the adsorption equilibrium:

$$q_t = q_e(1 - e^{-k_1 t}) \quad (5)$$

where q_t is the amount of Hg^{2+} adsorbed at time t (mg g^{-1}); q_e is the experimental amount of Hg^{2+} adsorbed at equilibrium (mg g^{-1}); and k_1 (min^{-1}) is the rate constant of the pseudo-first-order adsorption. The adsorption rate constant (k_1) and correlation coefficient (r^2) were calculated from the nonlinear plot of q_t versus t (Fig. 9a). The results are shown in Table 2. It can be seen from Fig. 9a that the correlation coefficient for the pseudo-first-order kinetic model was very high. However, there was a large difference in q_e between the experimental and calculated values, suggesting a poor fit for the pseudo-first-order kinetic model to the experiment data.

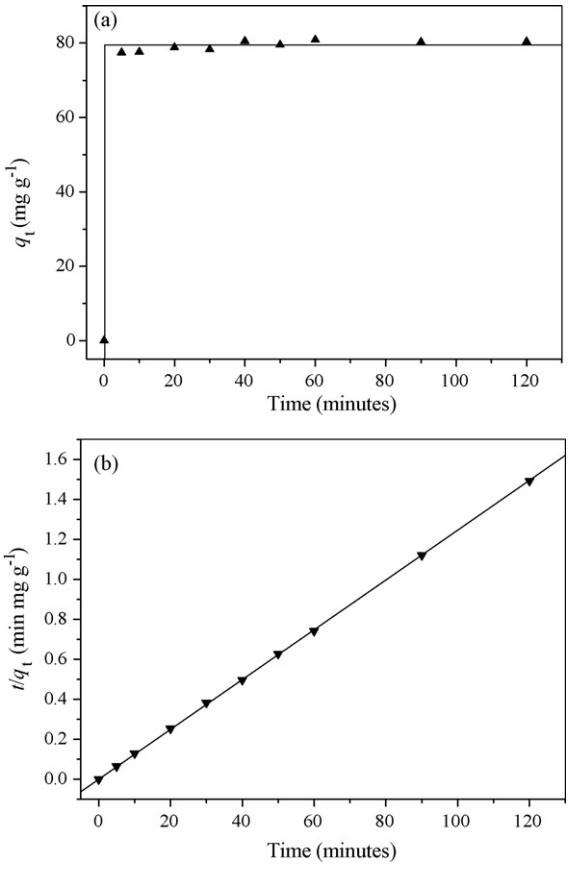

Fig. 9. The pseudo-first-order kinetics (a) and the pseudo-sencond-order kinetics (b) for the adsorption of Hg^{2+} onto PAM/ATP.

The rate constant for pseudo-second-order adsorption could be obtained from the following equation [36]:

$$\frac{t}{q_t} = \frac{1}{k_2 q_e^2} + \frac{t}{q_e} \quad (6)$$

where q_t is the amount of Hg^{2+} adsorbed at time t (mg g^{-1}); q_e is the experimental amount of Hg^{2+} adsorbed at equilibrium (mg g^{-1}); and k_2 (g mg^{-1} min^{-1}) is the rate constant of the pseudo-second-order adsorption. Fig. 9b presents the plot of (t/q_t) versus t for the adsorption of Hg^{2+} onto PAM/ATP. The k_2, the calculated q_e value and the correlation coefficient r^2 are given in Table 2. An extremely high correlation coefficient (0.999) was obtained. Moreover, the calculated q_e value also agrees with the experimental data in the case of pseudo-second-order kinetics. This suggests that the adsorption data are well represented by pseudo-second-order kinetics. Pseudo-second-order adsorption has also been reported for Hg^{2+} adsorption onto magnetically modified yeast cells [5]. These results also suggested that the pseudo-second-order mechanism is predominant and that the behavior over a whole range of adsorptions is in agreement with chemical adsorption, which is the rate-controlling step [37,38].

Table 2
Parameters of kinetic models of Hg^{2+} adsorption onto PAM/ATP.

Pseudo-first-order			Pseudo-second-order			Intraparticle diffusion		
q_e (mg g^{-1})	k_1 (min^{-1})	r^2	q_e (mg g^{-1})	k_2 (g mg^{-1} min^{-1})	r^2	K_i (mg g^{-1} $h^{-1/2}$)	C (mg g^{-1})	r^2
79.32	26.97	0.998	80.71	0.037	0.999	0.3990	22.21	0.698

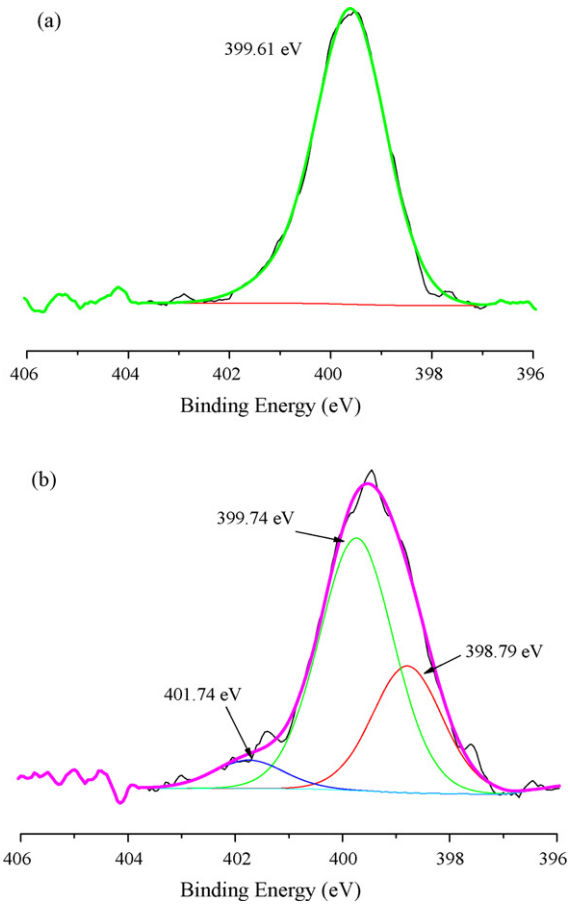

Fig. 10. XPS N 1s spectra of PAM/ATP: (a) before Hg^{2+} adsorption; and (b) after Hg^{2+} adsorption.

In addition, the kinetic data can also be analyzed by an intraparticle diffusion kinetics model, formulated as [39]:

$$q_t = k_i t^{1/2} + C \quad (7)$$

where k_i (mg g^{-1} h$^{-1/2}$) is the intraparticle diffusion rate constant and C (mg g^{-1}) is a constant. The values k_i, C and correlation coefficient r^2 calculated from the plot of q_t versus $t^{1/2}$ are shown in Table 2. It can be seen clearly from Table 2 that the correlation coefficient (r^2 = 0.698) for intraparticle diffusion is lower than those for the pseudo-first-order and pseudo-second-order models. This indicates that the intraparticle diffusion model does not explain the experimental data. In addition, it is necessary to note that the intercept (C) as proposed by Eq. (7) was not zero, but was a large value (22.21 mg g^{-1}), indicating that intraparticle diffusion is unlikely to be the controlling factor in determining the kinetics of the process [40].

The above results suggest that Hg^{2+} adsorption onto PAM/ATP was mainly dependent on chemical adsorption mechanisms (Eq. (8) or Eq. (9)), along with a contribution from cation exchange mechanisms (Eq. (10)).

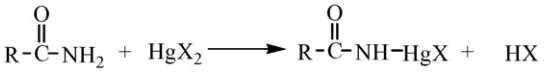

(8)

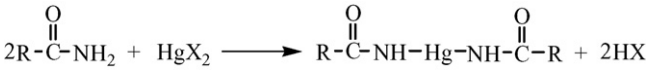

(9)

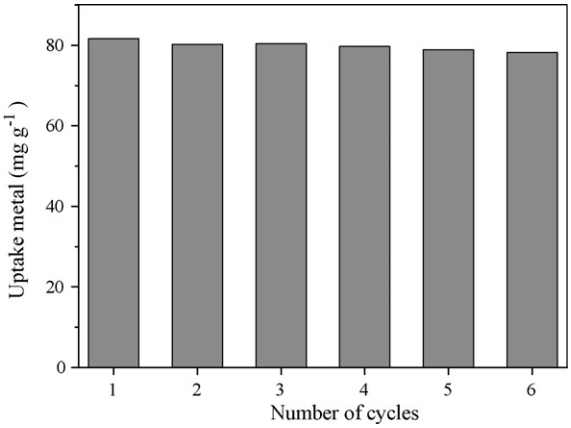

Fig. 11. Regeneration studies of PAM/ATP after six cycles.

$$\text{Clay}M^{n+} + Hg^{2+} \leftrightarrow \text{Clay}Hg^{2+} + M^{n+} \ (M = Na, K, Ca, Mg, etc.) \quad (10)$$

3.3. Mechanism of adsorption

To provide evidence for the adsorption mechanism, XPS analyses were conducted for PAM/ATP before and after Hg^{2+} adsorption at pH 4.4. Fig. 10 shows the typical N 1s XPS spectra of PAM/ATP with and without adsorbed Hg^{2+}. Before Hg^{2+} adsorption, there is only one peak in the N 1s spectrum at a BE of about 399.61 eV (Fig. 10a). This peak can be attributed to the nitrogen atoms in the amide groups in the grafted PAM. After Hg^{2+} adsorption, however, three peaks appeared in the N 1s spectrum (Fig. 10b). The new peak at a BE of 401.74 eV may be due to the formation of metal–NH_2 complexes for Hg^{2+}, but the intensity of this peak was very small, indicating that the amount of metal–NH_2 complex, if present, is very limited. The intensity of the new peak at a BE of 398.79 eV, however, was very strong, indicating that many nitrogen atoms existed in a more reduced state on the surface of PAM/ATP because of the metal adsorption. This was caused by the formation of a covalent bond of amido-Hg, in which Hg^{2+} shared electrons with the nitrogen atom in the O=C–NH_2 group, and as a consequence, the electron cloud density of the nitrogen atom was increased, resulting in a lower BE peak. The XPS results thus provide evidence to support an adsorption mechanism of covalent bonds formed between Hg^{2+} and amide groups.

3.4. Regeneration

We also studied the regeneration of the adsorbed Hg^{2+} ions from the PAM/ATP in a batch experimental set-up. We used hot acetic acid for extraction of the sorbed Hg^{2+}-loaded samples for 30 min. After washing with excess water, the adsorbents were available for re-use. The Hg^{2+} adsorption capacity of PAM/ATP is illustrated in Fig. 11 and was barely affected after six cycles. The adsorption capacity of the recycled the PAM/ATP was maintained at 95% by the sixth cycle. These results indicate that PAM/ATP is suitable for the enhanced removal of Hg^{2+} from wastewater.

4. Conclusions

PAM can be successfully grafted onto KH-570-modified ATP using the solution polymerization method, for enhanced removal of Hg^{2+} from aqueous solution. The adsorption capacity of Hg^{2+} onto the PAM/ATP increases with increasing contact time and pH of the initial suspension, but decreases with adsorbent dosage. Moreover, the amount of Hg^{2+} adsorbed per unit weight of ATP is less than that for PAM/ATP at pH 4.40. The results also showed that

PAM/ATP adsorbed Hg^{2+} very rapidly. The equilibrium data fitted the Langmuir sorption isotherm well, and the maximum adsorption capacity of Hg^{2+} onto PAM/ATP was 192.5 mg g^{-1}. The kinetics of Hg^{2+} adsorption onto PAM/ATP was based on the assumption of a pseudo-second-order mechanism, which is an important process in chemisorption. The higher adsorption capacity of PAM/ATP compared with ATP may be attributed to the ability of Hg^{2+} to form covalent bonds with the amide groups. Desorption was performed using hot acetic acid, and the regenerated adsorbents could be reused with little loss of adsorption capacity.

Acknowledgments

The authors are grateful for the financial support of the National Natural Science Fundation of China (20776067), Qing Lan Project and Natural Science Fundation of Jiangsu Education Department (07KJA15012, 08KJD530002), and the Program for Science and Technology Development of Huaian (HAG08041).

References

[1] R.P. Mason, J.R. Reinfelder, F.M.M. Morel, Uptake, toxicity, and trophic transfer of mercury in a coastal diatom, Environ. Sci. Technol. 30 (1996) 1835–1845.
[2] E.P.C. Lai, B. Wong, V.A. Vandernoot, Preservation of solid mercuric dithizonate samples with polyvinyl chloride for determination of mercury(II) in environmental waters by photochromism-induced photoacoustic spectrometry, Talanta 40 (1993) 1097–1105.
[3] J.R. Liu, K.T. Valsaraj, I. Devai, R.D. DeLaune, Immobilization of aqueous Hg(II) by mackinawit (FeS), J. Hazard. Mater. 157 (2008) 432–440.
[4] M.M. Matlock, B.S. Howerton, J.D. Robertson, D.A. Atwood, Gold ore column studies with a new mercury precipitant, Ind. Eng. Chem. Res. 41 (2002) 5278–5282.
[5] H. Yavuz, A. Denizli, H. Güngünes, M. Safarikova, I. Safarik, Biosorption of mercury on magnetically modified yeast cells, Sep. Purif. Technol. 52 (2006) 253–260.
[6] J. Barron-Zambrano, S. Laborie, Ph. Viers, M. Rakib, G. Durand, Mercury removal and recovery from aqueous solutions by coupled complexation-ultrafiltration and electrolysis, J. Membr. Sci. 229 (2004) 179–186.
[7] A.E. Gash, A.L. Spain, L.M. Dysleski, C.J. Flaschenriem, A. Kalaveshi, P.K. Dorhout, S.H. Strauss, Efficient recovery of elemental mercury from Hg(II)-contaminated aqueous media using a redox-recyclable ion-exchange material, Environ. Sci. Technol. 32 (1998) 1007–1012.
[8] M. Huebra, M.P. Elizalde, A. Almela, Hg(II) extraction by LIX 34. Mercury removal from sludge, Hydrometallurgy 68 (2003) 33–42.
[9] W.F. Bradley, The structure scheme of attapulgite, Am. Mineral. 25 (1940) 405–410.
[10] A. Neaman, A. Singer, Possible use of the Sacalum (Yucatan) palygorskite as drilling muds, Appl. Clay Sci. 25 (2004) 121–124.
[11] E. Álvarez-Ayuso, A. García-Sánchez, Removal of cadmium from aqueous solutions by palygorskite, J. Hazard. Mater. 147 (2007) 594–600.
[12] J.H. Potgieter, S.S. Potgieter-Vermaak, P.D. Kalibantonga, Heavy metals removal from solution by palygorskite clay, Miner. Eng. 19 (2006) 463–470.
[13] H. Chen, Y.G. Zhao, A.Q. Wang, Removal of Cu(II) from aqueous solution by adsorption onto acid-activated palygorskite, J. Hazard. Mater. 149 (2007) 346–354.
[14] W.J. Wang, H. Chen, A.Q. Wang, Adsorption characteristic of Cd(II) from aqueous solution onto activated palygorskite, Sep. Purif. Technol. 55 (2007) 157–164.
[15] E. Galan, Properties and applications of palygorskite-sepiolite clays, Clay Miner. 31 (1996) 443–453.
[16] H.H. Murray, Traditional and new applications for kaolin, smectite, and palygorskite: a general overview, Appl. Clay Sci. 17 (2000) 207–211.
[17] P. Liu, T.M. Wang, Adsorption properties of hyperbranched aliphatic polyester grafted ATP towards heavy metal ions, J. Hazard. Mater. 149 (2007) 75–79.
[18] J.H. Huang, Y.F. Liu, X.G. Wang, Selective adsorption of tannin from flavonoids by organically modified attapulgite clay, J. Hazard. Mater. 160 (2008) 382–387.
[19] Q.H. Fan, D.D. Shao, J. Hu, W.S. Wu, X.K. Wang, Comparison of Ni^{2+} sorption to bare and ACT-graft ATPs: Effect of pH, temperature and foreign ions, Surf. Sci. 602 (2008) 778–785.
[20] N. Li, R.B. Bai, C.K. Liu, Enhanced and selective adsorption of mercury ions on chitosan beads grafted with polyacrylamide via surface-initiated atom transfer radical polymerization, Langmuir 21 (2005) 11780–11787.
[21] H. Bulbul Sonmez, B.F. Senkal, D.C. Sherrington, N. Bicak, Atom transfer radical graft polymerization of acrylamide from N-chlorosulfonamidated polystryrene resin, and use of the resin in selective mercury removal, React. Funct. Polym. 55 (2003) 1–8.
[22] G.N. Manju, K. Anoop Krishnan, V.P. Vinod, T.S. Anirudhan, An investigation into the sorption of heavy metals from wastewaters by polyacrylamide-grafted iron(III) oxide, J. Hazard. Mater. B91 (2002) 221–238.
[23] H. Bulbul Sonmez, B.F. Senkal, N. Bicak, Poly(acrylamide) grafts on spherical bead polymers for extremely selective removal of mercuric ions from aqueous solutions, J. Polym. Sci.: Polym. Chem. 40 (2002) 3068–3078.
[24] N. Bicak, D.C. Sherrington, B.F. Senkal, Graft copolymer of acrymamide onto cellulose as mercury selective sorbant, React. Funct. Polym. 41 (1999) 69–76.
[25] I.G. Shibi, T.S. Anirudhan, Synthesis, characterization, and application as a mercury(II) sorbent of banana stalk (Musa paradisiaca) polyacrylamide grafted copolymer bearing carboxyl groups, Ind. Eng. Chem. Res. 41 (2002) 5341–5352.
[26] P. Liu, J.S. Guo, Polyacrylamide grafted attapulgite (PAM-ATP) via surface-initiated atom transfer radical polymerization (SI-ATRP) for removal of Hg(II) ion and dyes, Colloids Sur. A: Physicochem. Eng. Aspects 282–283 (2006) 498–503.
[27] A. Li, R.F. Liu, A.Q. Wang, Preparation of starch-graft-poly(acrylamide)/attapulgite superabsorbent composite, J. Appl. Polym. Sci. 98 (2005) 1351–1357.
[28] R.G. Pearson, Hard and soft acids and bases, J. Am. Chem. Soc. 85 (1963) 3533–3539.
[29] J. Choong, H.H. Wolfgang, Chemical modification of chitosan and equilibrium study for mercury ion removal, Water Res. 37 (2003) 4770–4780.
[30] R.R. Navarro, K. Sumi, N. Fujii, M. Matsumara, Mercury removal from wastewater using porous cellulose carrier modified with polyethyleneimine, Water Res. 30 (1996) 2488–2494.
[31] X. Zhang, R.B. Bai, Deposition/adsorption of colloids to surface-modified granules: effect of surface interactions, Langmuir 18 (2002) 3459–3465.
[32] I. Langmuir, The adsorption of gases on plane surfaces of glass, mica and platinum, J. Am. Chem. Soc. 40 (1918) 1361–1403.
[33] A.A. Asem, Studies on the interaction of mercury(II) and uranyl(II) with modified chitosan resins, Hydrometallurgy. 80 (2005) 13–22.
[34] M. Ahmaruzzaman, D.K. Sharma, Adsorption of phenols from wasterwater, J. Colloid Interface Sci. 287 (2005) 14–24.
[35] S. Lagergren, About the theory of so-called adsorption of soluble substances, Kungliga Svenska Vetenskapsakademiens, Handlingar 24 (4) (1898) 1–39.
[36] Y.S. Ho, G. Mckay, Pseudo-second order model for sorption processes, Process Biochem. 34 (1999) 451–465.
[37] E. Guibal, C. Milot, J.M. Tobin, Metal-anion sorption by chitosan beads: equilibrium and kinetic studies, Ind. Eng. Chem. Res. 37 (1998) 1454–1463.
[38] P. Baskaralingam, M. Pulikesi, D. Elango, V. Ramamurthi, S. Sivanesan, Adsorption of acid dye onto organobentonite, J. Hazard. Mater. 128 (2006) 138–144.
[39] W.J. Weber Jr., J.C. Morriss, Kinetics of adsorption on carbon from solution, J. Sanitary Eng. Div. Am. Soc. Civ. Eng. 89 (1963) 31–60.
[40] H. Chen, A.Q. Wang, Kinetic and isothermal studies of lead ion adsorption onto palygorskite clay, J. Colloid Interface Sci. 307 (2007) 309–316.